AMERICAN JOURNAL OF BIOCHEMISTRY AND BIOTECHNOLOGY

RESEARCH ARTICLE

Cytocompatibility and Antimicrobial Properties of Silver Nanoparticles-Loaded AMPs in the Oral Cavity

Yanli Lv*, Weikai Zhang

Luoyang Polytechnic, Luoyang 471000, China

*Corresponding Author: lylyl186@126.com

Abstract: Postoperative infection following oral metal implantation is a key factor that affects the success rate of surgery. This infection is mainly caused by bacterial biofilms. Traditional single antibacterial coatings have limitations, including a narrow antibacterial spectrum and poor cytotoxicity or stability. This study combined silver nanoparticles (AgNPs) and the synthetic antimicrobial peptide GL13K using electrostatic self-assembly technology to create a dual-effect antimicrobial coating. The AgNPs were prepared using the chemical reduction method, and the GL13K nanofibers were formed through β-folding self-assembly. These processes utilized their complementary charge characteristics to achieve a precise composite. The experimental results showed that the antibacterial rate of the coating against streptococcus pneumoniae, pseudomonas aeruginosa, and MRSA was significantly higher than that of a single coating (reducing CFU by 2-3 orders of magnitude, $p<0.01$). Moreover, the minimum inhibitory concentration (MIC) decreased to 1.0±0.3 μ g/mL (synergistic index 0.28). In the dynamic oral environment simulation experiment, the coating exhibited high antibacterial activity at a saliva flow rate of 0.25 mL/min. Cell experiments confirmed that it had no effect on the activity of human bone marrow mesenchymal stem cells ($p>0.05$). The effect of different nanoconcentrations and coating temperature on antibacterial activity was not statistically significant ($p>0.05$). This study addresses the limitations of traditional coatings by using a collaborative, nanoscale design approach to provide a new strategy for optimizing the antibacterial properties of oral implant materials.

Keywords: Oral Metal Implants; Antimicrobial Coatings; Synthetic Antimicrobial Peptides; Cytocompatibility; Silver Nanoparticles

Received: 30-04-2025 | **Revised:** 18-06-2025 | **Accepted:** 18-11-2025 | **DOI:** 10.3844/ajbbsp.2026.22.01.015

Introduction

Oral metal implantation surgery is an important means of modern dental restoration and treatment. However, postoperative infection remains a key factor affecting surgical success rate and patient prognosis [1]. Bacterial biofilms are considered the main cause of implant infections. Their complex structure allows bacteria to resist the host immune system and the effects of antibiotics. This enables them to survive on implant surfaces for extended periods and trigger inflammatory reactions [2, 3]. Silver nanoparticles (AgNPs) and antimicrobial peptides (AMPs) have antibacterial properties, but they are limited when used alone. For example, AgNPs are ineffective against Gram-negative bacteria, and high concentrations of AgNPs are cytotoxic. Natural AMPs are easily degraded by proteases and costly [4, 5]. More importantly, existing coatings often rely on simple physical mixing. This method fails to take advantage of the two components' synergistic effect and

precisely locate AgNPs on the AMP molecular structure. The result is low antibacterial efficiency and issues with the release of silver ions. Additionally, the combination of AgNP and GL13K has an advantage over existing antibacterial methods. This is because it takes advantage of the complementary charge characteristics between the polar end of the GL13K AMP and the surface of the AgNP. This allows for precise nanoscale positioning through electrostatic self-assembly. This combination of methods solves the problem of uneven AgNP distribution in traditional blending. In addition, a postoperative infection can directly affect the stability and functional recovery of the implant. It can also significantly reduce a patient's chewing efficiency and oral comfort. In severe cases, it can cause the implant to loosen or even fall out, thereby having a negative impact on the patient's mental health and social interaction. Once an infection occurs, multiple debridements, antibiotic treatments, and sometimes even secondary surgeries to replace the implant are often required. This significantly increases the treatment cycle and medical costs, imposing a heavy burden on patients and the medical system. Even more importantly, infection can cause local bone tissue resorption and chronic inflammation. It can also lead to systemic infection, which affects patients' long-term prognosis and quality of life. Therefore, developing a surface coating for implants that combines highly efficient antibacterial performance with good biocompatibility is clinically significant and valuable in reducing postoperative infection rates, increasing implant success rates, and alleviating patient suffering and economic burden.

Numerous scholars have conducted in-depth analysis and exploration on this matter. Grachev et al. aimed to create and implement a new model for evaluating the socioeconomic feasibility of investing in digital technology for diagnosing and treating patients who were completely edentulous and had removable polymer dentures that were manufactured via 3D additive printing [6]. The results showed that this method could provide a basis for the selection of denture restoration techniques for patients with complete dentition loss, thereby achieving the most rational utilization of resources. Snauwaert & Vanhoucke found that AMPs exhibited antimicrobial and immunomodulatory activities that helped to control periodontitis [7]. It also analyzed the immunopathological role of Porphyromonas gingivalis-activated macrophages in periodontitis. Therefore, this study suggested AMPs as a treatment for periodontitis. To improve the antibacterial and anti-biofilm properties of AgNPs, Abdallah et al. prepared an orthodontic wire wrapped coating by combining it with nanocomposites [8]. The coating was found to exhibit significant antibacterial and anti-biofilm activity against normal flora and multidrug resistant bacteria. Elchaghaby et al. explored the antimicrobial effect of AgNPs biosynthesized from aniseed against streptococcus pyogenes [9]. It was found that AgNPs had high antioxidant activity. Furthermore, they effectively inhibited the growth of streptococcus pyogenes, producing an inhibition zone diameter of 16 mm and a minimum inhibitory concentration (MIC) of 80 μg/mL. The above methods relied on oxidative stress and lacked specificity. This study used GL13K β-folded nanofibers to provide ordered assembly templates, employing a sustained-release design to extend the action time. This improved the methods' clinical applicability. Garibay-Alvarado et al. synthesized a resin containing hydroxyapatite and AgNP to enhance its biocompatibility and antimicrobial efficacy for use in dental restorations to reduce bacterial colonization [10]. The resin was found to have bactericidal properties against a wide range of bacteria, with significant inhibition achieved at low silver concentrations. The above study used a single AgNP coating that exhibited high-dose toxicity and had a poor effect on Gram-negative bacteria, resulting in a cell survival rate of less than 70%. However, this study proposed using an electrostatic programming assembly strategy to achieve enhanced antibacterial properties.

In summary, the application of AMPs and AgNP can reduce infection, inflammation and pain to a certain extent, and has a significant inhibitory effect on bacteria. However, when AMPs or AgNP are used alone, there may be problems such as limited antimicrobial effect, increased drug resistance or poor cytocompatibility. The composite use of AMPs, AgNP and other materials has become a new direction of research. However, the use of AMPs in combination with AgNP to optimize the performance of anti-infective coatings has yet to be verified. Therefore, the goal is to overcome the shortcomings of existing antimicrobial coatings and provide an efficient, reliable, and safe solution for preventing infections after oral metal implant surgery. This study innovatively constructs a dual coating of AgNP-loaded AMPs. It focuses on the coating's cytocompatibility and antimicrobial properties in the oral cavity. The study aims to provide a solid theoretical basis and experimental data to support the clinical application of the coating in the oral cavity. This study has been approved by the hospital ethics committee.

Materials and Methods

Laboratory Materials

The AMPs selected for the study are GL13K, which is a novel AMP obtained by modification and optimization of natural AMPs. Combining AgNP with GL13K enables them to maximize their antimicrobial properties, creating a composite material with enhanced antimicrobial activity. This principle is consistent with findings showing that incorporating AgNPs into composite

systems, such as AgNP-loaded PVA hydrogels, produces powerful bactericidal effects against both gram-positive and gram-negative bacteria that surpass those of AgNPs applied individually [11-13]. The synthesis process of the two is shown in Fig. 1.

The work employs the self-assembly process to create positively charged nanofibers from the GL13K molecular structure, as shown in Fig. 1. Then, it combines the negatively charged AgNP with positively charged GL13K nanofibers by using the electrostatic attraction between positive and negative charges. Finally, the titanium-based surface is treated by alkaline etching to form a coating by tightly binding it with GL13K and AgNP.

Synthesis of AgNP

Preparation of AgNP: AgNP is synthesized by chemical reduction method in the study. 0.1699g of silver nitrate solid is dissolved in 10mL of deionized water and transferred to a 100mL volumetric flask to be fixed to formulate the silver source solution with 0.1mol/L concentration. The solution of sodium borohydride reducing agent at a concentration of 0.1 mol/L, and polyvinylpyrrolidone stabilizer at 0.005 g/mL are also configured in the same manner. Then, 0.1 mol/L silver ion solution is added to the beaker and the reducing agent solution is added slowly while stirring. The reaction solution is placed in a temperature-controlled water bath and reacted at 40°C for 30-60 mi [14, 15].The final AgNP solutions of 0.2 mg/mL, 1 mg/mL, and 5 mg/mL are prepared

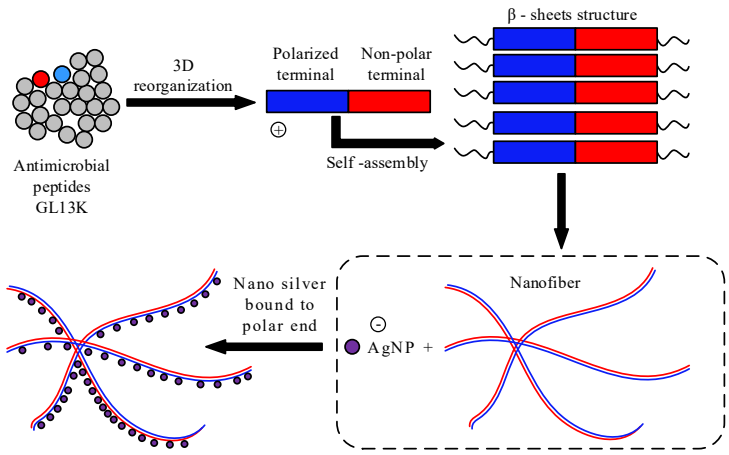

Fig. 1: Schematic Diagram of the Complexation Process of AgNP with GL13K. Nanofibers form through the self-assembly of β-folded structures. The surfaces of AgNPs carry negative charges and selectively bind to the polar end of GL13K through electrostatic interactions. Finally, a composite structure of AgNP nanofibers is formed, with AgNPs regularly distributed at the polar ends of the fibers

GL13K solution preparation: A solution of 100 mg/mL is prepared by adding AMP GL13K to deionized water and stirring until completely dissolved. Subsequently, 10 µL of GL13K is added to 990 µL of borax-sodium hydroxide buffer to prepare a 1 mg/mL solution of GL13K. Moreover, the dissolved AMP GL13K solution is filtered through a 0.45 µm aqueous filtration membrane to remove insoluble matter to obtain a clarified AMP GL13K solution. Finally, the filtered AMP GL13K solution is stored at 4°C to ensure the activity and stability of AMP [16, 17]. Finally, the prepared AgNP solution is mixed with GL13K solution and stored at 4°C as well as at room temperature. It is self-assembled into nanofibers to form self-assembled structures with antimicrobial activity.

Construction of AgNP-GL13K Coating

AgNP-GL13K complex coating: Pure titanium is first punched to make a titanium sheet, and sandpaper is used to smooth it out. The titanium sheet is immersed in acetone and ultrasonically cleaned for 15 min to remove organic contaminants from the surface. Subsequently, the cleaned titanium sheet is submerged in a sodium hydroxide solution with a pH of 9.8 for an alkaline etching treatment. This treatment increases the roughness and activity of the titanium sheet's surface, which improves adhesion of subsequent coatings. Finally, the cleaned titanium sheets are dried in an oven at 60°C. The finished AgNP-GL13K mixture is slowly added to the surface of the pretreated titanium sheets to ensure uniform adhesion [18]. Finally, the titanium sheets are coated with the complex solution and dried naturally at room temperature, forming a stable AgNP-GL13K coating.

The materials and reagents used in this study include: silver nitrate (product number 7761-88-8, Guangdong Xianglong Chemical), sodium borohydride (16940-66-2, Maoming Xiongda Chemical), polyvinylpyrrolidone (9003-39-8, Sigma Aldrich), pure titanium sheet (TC4, Jiangsu Jiuming Special Steel), AMP GL13K (GKIIKLKASL-NH2, AAPPTEC USA), borax (1303-96-4, Chengdu Zhongpeng Chemical), sodium hydroxide (1310-73-2, Anhui Jingyueguan New Materials), and acetone (119-51, Hubei Keji Biopharmaceutical). To ensure the reliability and reproducibility of the experimental materials, all of the reagents are sourced from well-known domestic and international manufacturers.

After the experiments are finished, morphological, structural, and elemental analyses are performed, followed by surface property evaluations, to fully characterize the physicochemical properties. Morphological analysis: The micro-morphology of AgNP-GL13K complex is observed with the help of Transmission Electron Microscope (TEM) to evaluate the distribution of AgNP particles and GL13K nanofibers on the surface of titanium sheets. The titanium sheet microcosmography is also observed with the help of Scanning Electron Microscope (SEM). Structural analysis: The secondary structure changes of GL13K in the coating are analyzed using Circular Dichroism (CD) to evaluate its self-assembly behavior. Elemental analysis: The elemental composition of the coating surface is analyzed by X-ray Photoelectron Spectroscopy (XPS) to confirm the successful coating of AgNP and GL13K. Surface property assessment: The hydrophilicity of the coating surface is measured using Water Contact Angle (WCA) to assess its effect on bacterial adhesion.

The experimental equipment mainly includes: magnetic stirrer (WH280-NH, Weigen Technology), centrifuge (TG16G, Shandong Sanyi Instrument), constant temperature water bath (JZSY-100, Zhengzhou Jingzhong Instrument), ultrasonic cleaning machine (SUI-230T, Shanghai Puyu Industry), CD spectrometer (Jasco J-815, Japan Jasco), X-ray photoelectron spectrometer (Nexsa G2, Thermo Fisher), contact angle measuring instrument (CA200, Beidou Instrument), and vacuum drying oven (ST-10N-60D, Shandong Sanyi Instrument).

In Vitro Antimicrobial Studies in a Static Environment

The antimicrobial activity of the coating against S. gordonii gram-positive streptococcus is firstly explored. S. gordonii is selected as the research object, and it is inoculated on agar medium and statically incubated at 37°C for 6h to reach the logarithmic growth period. Twelve coated titanium flakes with different temperature and concentration combinations are obtained by combining 0.2 mg/mL, 1 mg/mL, and 5 mg/mL of AgNP solution with GL13K solution at 4°C and room temperature conditions. Subsequently, cultured S. gordonii is co-incubated with the coated titanium sheets for a certain period of time to evaluate the effect of the coating on bacterial activity. Adenosine triphosphate (ATP) fluorescence assay is chosen for the study to detect the amount of ATP in bacteria to indirectly reflect the activity of bacteria. The ATP bioluminescence kit is used to detect the ATP content in the samples according to the instructions. The Colony Forming Unit (CFU) counting method is also used to determine CFU by plate counting method to directly reflect the number of live bacteria. The study is carried out by diluting the samples appropriately after co-incubation, spreading them on agar plates and counting the CFUs after incubation to directly assess the number of viable bacteria.

The study further selects Gram-negative bacteria P. aeruginosa, Methicillin-Resistant Staphylococcus Aureus (MRSA) for more in-depth in vitro antimicrobial resistance studies. After the blood agar plates inoculated with bacteria are placed in an incubator for 24h, single colonies of different strains of bacteria are formed on the plates. A certain number of single colonies are selected from the recovered strains and inoculated into 5mL nutrient broth medium respectively. Moreover, the bacteria are incubated overnight at 37°C and 180 rpm under an oscillating environment to reach the logarithmic growth phase. Finally, the bacteria that have been cultured overnight are inoculated into a fresh nutrient broth medium at a ratio of 1:100. The medium is then incubated at 37° C and 180 rpm in an oscillating environment until the OD600 reaches 0.6-0.8. The study is set up with four kinds of control titanium sheets, 0.2 mg/mL AgNP titanium sheets, GL13K-4°C titanium sheets, 0.2 mg/mLAgNP-GL13K-4°C titanium sheets different coatings. CFU is used for bacterial enumeration.

Antimicrobial Properties in an in Vitro Simulated Oral Environment

To investigate the antimicrobial performance of AgNP-GL13K composite coated titanium sheets in a simulated oral environment, this study sets up four different coatings, control titanium sheets, 0.2 mg/mL AgNP titanium sheets, GL13K-4°C titanium sheets, and 0.2 mg/mLAgNP-GL13K-4°C titanium sheets, and simulated them in a drip-flow bioreactor. The early colonization of bacteria is formed by culturing the S. gordonii strain (ATCC 10558). Meanwhile, P. aeruginosa (ATCC 27853) is also used. These strains are immobilized in the reactor's channel, which is tilted to ensure uniform flow of the culture solution through the sample. Subsequently, the bioreactor is heated with broth medium to 37°C to simulate oral temperature. Broth medium at 37°C is pumped into the bioreactor at a flow rate of 0.25 mL/min with the help of a peristaltic pump to simulate the

flow rate of oral saliva. The culture is continuously incubated for 48h under the condition of simulated saliva flow to promote biofilm formation and further colonization of bacteria. At the end of the incubation the titanium slice samples are removed from the bioreactor and gently rinsed with phosphate buffer to remove uncolonized bacteria [19]. The antimicrobial performance of AgNP-GL13K composite-coated titanium sheets in a simulated oral environment was evaluated using the methodology of static antimicrobial experiments as a reference.

In Vitro Antibacterial Activity Analysis

The in vivo biological environment involves complex physiological and immune responses. The study further evaluates the antimicrobial performance of the coating against MRSA by establishing a rat model. Sprague-Dawley rats from the Animal Experiment Center of Wuhan University are chosen as experimental animals to establish the MRSA infection model. First, the culture of bacteria is completed with reference to the antimicrobial property study of MRSA in static environment in vitro. Then, male rats of 10 weeks of age/weight 300-400 g are selected and individually acclimatized and fed for one week to start the experiment, which is reviewed and approved by the Ethics Committee. The study sets up four different coatings: control titanium sheet, 0.2mg/mL AgNP titanium sheet, GL13K-4°C titanium sheet, and 0.2mg/mLAgNP-GL13K-4°C titanium sheet. Healthy, weight-adapted rats are selected for the experiment and randomly numbered after preoperative weighing. The implant is sterilized according to experimental requirements to ensure the number and activity level of MRSA bacteria meet those requirements. The anesthesia of the rats is completed by intraperitoneal injection of the animals, and the sterilized samples are implanted into subcutaneous pouches. Moreover, the MRSA bacterial suspension is injected into the subcutaneous pouch around the implant through an appropriate route. After completion of the procedure, the wound is sutured and necessary postoperative care is given.

Five days after implantation, the rats are euthanized and the titanium pieces are removed. The pieces are then subjected to bacterial staining and CFU analysis using appropriate methods, in accordance with animal ethics and experimental norms. The surface of the titanium sheet is gently washed with sterile phosphate buffer after removal to remove impurities such as blood and tissue fragments adhering to the surface. The cleaned titanium slice is immersed in 1 ml of sterile phosphate buffer, ensuring that the titanium slice is completely submerged. The appropriate amount of stain is prepared according to the live/dead bacterial staining kit instructions. The titanium slice is removed from the phosphate buffer and a drop of stain is added to the surface of the titanium slice. Subsequently, incubation is performed according to the kit instructions to allow the stain to fully bind to the bacteria on the surface of the titanium slice. Finally, a fluorescence microscope is used to observe the fluorescence signal on the surface of the titanium slice.

Mesenchymal Stem Cell Culture

To investigate whether the coating affects host cell adhesion and proliferation, the study is performed to analyze cytocompatibility. First, the culture of human bone marrow mesenchymal stem cells is established. In the study, high-sugar DMEM was chosen as the basal medium for human bone MSCs. Moreover, 1 ng/mL of basic fibroblast growth factor is added to promote cell proliferation and differentiation. Fetal bovine serum is added to a final concentration of 10% to provide nutrients and growth factors for cell growth. The temperature of the incubator is maintained at 37°C and the humidity is kept at 70%-80% to simulate the microenvironment of cell growth in vivo. First, the frozen storage tubes containing human bone marrow mesenchymal stem cells are thawed by rapid shaking in a 37°C water bath. The appropriate amount of culture medium is added and mixed well, and then centrifuged to remove the supernatant. Moreover, the cells are resuspended with culture medium and transferred to culture dishes for overnight incubation. When the cell density reaches 80%-90%, passaging culture is performed. Finally, the cells are inoculated on the surface of the samples, and the adhesion and spreading of the cells are determined periodically.

Determination of Cell Proliferative Capacity

The study determines the amount of cell proliferation using CCK-8 kit. First, cells are inoculated into 96-well plates and incubated at 37°C, 5% CO_2, and 90% humidity for a period of time to allow the cells to attach to the wall and proliferate. Subsequently, 10 μL of CCK-8 solution is added to each well at the indicated time points. The incubation is also continued for 4h to allow WST-8 to be reduced by intracellular dehydrogenase. Finally, the absorbance value of each well is measured at 450 nm using an enzyme marker. Meanwhile, the detection wavelength of 450-490 nm and the reference wavelength of 600-650 nm are determined in order to more accurately assess the cell proliferation.

Methods of Statistical Analysis

DOI: 10.3844/ajbbsp.2026.22.01.015

The experimental data are processed and analyzed using SPSS 24.0 and Excel software. The measurement data are presented as “mean±standard deviation”. The study sets the significance level $\alpha = 0.05$. When p<0.05, it means that the difference is statistically significant. When p<0.01, it means that the difference is statistically significant. The Kolmogorov-Smirnov (K-S) test is used for data that obeys a normal distribution, and a one-way ANOVA is used to compare differences between groups. Levene's test for chi-square is used for outliers or non-normally distributed data from multiple samples. The Dunnett T3 post hoc test is used to detect differences among groups. The K-S test method is primarily used to determine whether experimental data is normally distributed, ensuring the appropriate statistical methods are selected in the future. The Dunnett T3 test is used for pairwise comparisons of multiple sets of data, particularly when variances are heterogeneous. However, when the data does not satisfy the homogeneity of variance assumption, that is, when the Levene test is significant, the Dunnett T3 test is more suitable for handling such data because it does not rely on this assumption. The specific testing process is as follows: First, normality testing is performed using the K-S test to determine if the data follows a normal distribution. This helps decide if parametric or nonparametric testing should be used in the future. If the data are normally distributed, perform a homogeneity of variance test using the Levene method. Then, use the Dunnett T3 post hoc test to analyze intergroup differences.

Results

Nanofiber Characterization

The characterization of GL13K, AgNP-GL13K complexes and their coatings are shown in Fig. 2. Figs. 2(a) and (b) indicate that there is a significant difference in the self-assembly of nanofibers of GL13K at 4 °C and room temperature conditions. Fig. 2(a) illustrates the long, twisted structure of the nanofibers, which are less than 50 nm. In contrast, under room temperature conditions, the nanofibers are surrounded by more irregular nanosphere structures. Figs. 2(c) and (d) show that AgNP is distributed on top of the GL13K self-assembled structure. In addition, the titanium sheet in Fig. 2(e) shows a porous honeycomb structure after alkali etching, which creates a large number of microscopic holes or depressions. The surface area of its structure is expanded, enhancing its adsorption capacity and reactivity. The uniform distribution of AgNPs and the ordered structure of GL13K fibers promote the coating's efficient antibacterial performance. The precise positioning of the AgNPs increases their likelihood of coming into contact with bacterial cells. Meanwhile, the fiber structure of the GL13K provides a stable carrier and a synergistic antibacterial effect. The porous surface of the titanium sheet enhances both the adhesion of the coating and the sustained release of antibacterial components. This significantly improves the sheet's ability to inhibit bacterial biofilms.

Surface Chemistry

The CD spectra of GL13K and AgNP-GL13K complexes as well as the results of secondary structure analysis are shown in Fig. 3. In Fig. 3(a), there is a significant difference in the CD spectra of different structures at 4°C and room temperature. The temperature has an important effect on the formation and arrangement of its secondary structure. Fig. 3(b) shows the estimation results of the secondary structures. The β-folding structure is higher in GL13K and AgNP-GL13K. However, at lower temperatures, the molecular motion is slowed down. This favors the formation of more stable and ordered antiparallel β-folded structures, accounting for more than 20%.

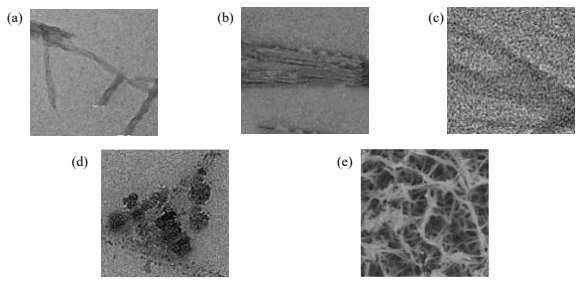

Fig. 2: Microscopic Characterization Image Analysis. (a) TEM image of GL13K self-assembled nanofibers at 4 ° C (scale: 200 nm). (b) TEM image of GL13K at room temperature, showing irregular nanosphere structure (scale: 100 nm). (c) Distribution of AgNP on GL13K nanofibers (scale: 50 nm). (d) High resolution TEM image of AgNP-GL13K complex (scale: 20 nm). (e) The SEM image of the titanium sheet surface after alkaline etching shows a porous honeycomb structure (scale: 5 μm). All images represent at least 5 independent experiments

DOI: 10.3844/ajbbsp.2026.22.01.015

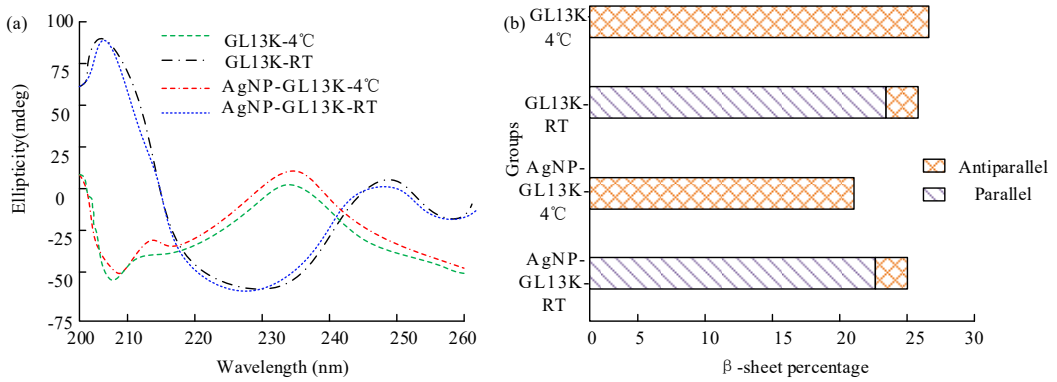

Fig. 3: CD Spectra and Secondary Structure Analysis of GL13K and AgNP-GL13K Complexes at 4 ℃ and Room Temperature. (a) Representative CD spectra of GL13K (blue) and AgNP-GL13K (red) at 4 ℃. (b) Percentage of β-sheet content as determined by spectral deconvolution. Data are shown as mean±SD (n=5). Statistical significance is assessed by unpaired t-test, *p*<0.05 compared to room temperature

In Vivo Testing

The XPS analysis results of AgNP-GL13K coatings are shown in Table 1. The presence of Ag element can be detected in different concentrations of AgNP coating and AgNP-GL13K coating. However, the Ag content and Ag/Ti ratio are relatively low. Only the Ag/Ti ratio of the AgNP coating with 5 mg/mL reaches 0.15, indicating that the AgNP content in the coating is not high. Nevertheless, the N/Ti and C/Ti values of GL13K and AgNP-GL13K coatings take a significant increase compared to Ti and AgNP coatings. The presence and distribution of GL13K coating on the surface of titanium is confirmed.

The results of the WCA analysis of the AgNP-GL13K coating are shown in Fig. 4. In Fig. 4(a), the surface WCA of the control Ti plate or the single AgNP coating is small, taking a value of about 20°, presenting a hydrophilic surface. As shown in Fig. 4(b), the WCA of the AgNP-GL13K coating is approximately 90° -100° . This significantly improves the surface properties of the titanium sheet, transforming it from hydrophilic to hydrophobic. The Ag/Ti ratio of all AgNP coating groups is relatively low, indicating that the actual loading of AgNP in the coating is not high. This suggests that efficient antibacterial activity can be achieved with low doses of AgNP through its synergistic effects with GL13K. This reduces the potential cytotoxicity risks associated with high silver concentrations. The low content of Na, Si, and Cl elements usually has no significant effect on the coating performance. As the coverage of organic coatings increases, the signal of the titanium substrate itself (the proportion of Ti and O elements) weakens. This is consistent with the increase in coating coverage. The presence of all three elements (Ag, N, and C) in the composite coating proves that the AgNP forms a composite structure with the GL13K rather than being a simple physical mixture. This precise nanostructure formed through electrostatic self-assembly is the key to exerting synergistic antibacterial effects. After the GL13K organic layer is successfully introduced, the coating surface's chemical properties undergo fundamental changes. Forming hydrophobic surfaces reduces non-specific protein adsorption and initial bacterial adhesion, which enhances the anti-biofilm performance of the coating.

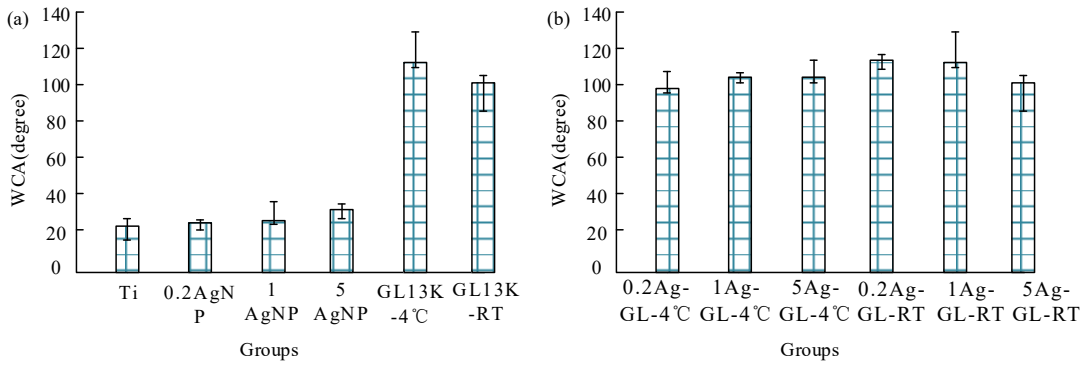

Fig. 4: WCA Analysis Results of Coatings. (a) Measurement of WCA (approximately 20 °) for the control group of titanium sheets and a single AgNP coating. (b) Contact angle distribution (90 °-100 °) of AgNP-GL13K coating. Each measurement should be repeated at least 5 times, and the data should be expressed as mean±SD

DOI: 10.3844/ajbbsp.2026.22.01.015

Table 1: XPS Analysis Results of Different Coatings

Group	/	Cls	Nls	Ols	Nals	Si2p	Cl2p	Ti2p	Ag3d	N/Ti	C/Ti	Ag/Ti
Ti	Mean	10.28	0.49	59.83	8.56	0.19	0.26	19.70	1.18	0.05	0.38	0.00
	SD	0.19	0.74	0.97	1.55	0.52	0.60	0.12	0.31	/	/	/
0.2AgNP	Mean	12.37	0.44	61.66	7.98	0.99	0.25	16.37	0.42	0.02	0.71	0.01
	SD	1.52	1.51	1.09	1.62	0.35	0.56	0.53	0.24	/	/	/
1AgNP	Mean	11.16	0.80	59.89	8.85	0.90	0.19	17.86	0.54	0.03	0.65	0.04
	SD	1.12	1.26	1.60	1.26	1.19	1.99	1.89	0.07	/	/	/
5AgNP	Mean	13.11	0.62	60.75	6.43	1.19	0.17	14.40	2.98	0.03	0.87	0.15
	SD	1.93	0.16	0.06	0.38	1.54	1.51	0.52	0.92	/	/	/
GL13K-4℃	Mean	48.75	11.62	28.79	4.94	0.45	0.02	6.85	0.05	1.81	8.83	0.01
	SD	1.45	1.65	0.98	1.53	0.95	1.93	0.76	0.37	/	/	/
GL13K-RT	Mean	41.04	9.25	36.76	4.21	0.53	0.13	8.03	0.06	1.11	4.65	0.05
	SD	0.27	1.38	0.12	0.32	0.21	1.16	1.32	1.78	/	/	/
0.2AgNP-GL13K-4℃	Mean	39.08	9.75	37.51	1.58	0.57	0.55	9.75	0.40	1.06	4.29	0.03
	SD	1.58	0.99	1.09	1.01	1.79	0.37	1.46	0.34	/	/	/

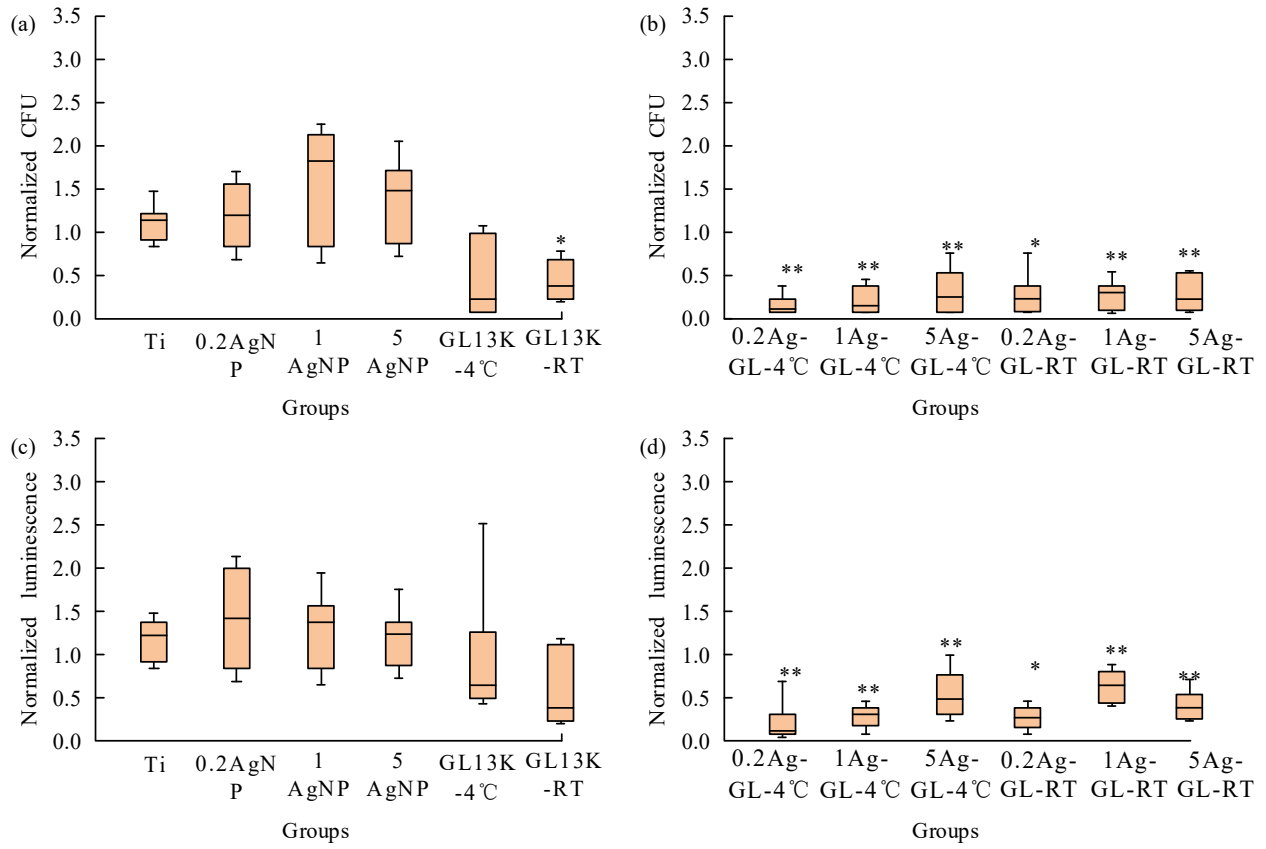

Fig. 5: In Vitro Antibacterial Activity Analysis. (a) Count of CFU of each coating under static cultivation (log10 converted data). (b) ATP bioluminescence intensity (relative fluorescence unit, RLU). (c) Comparison of CFU of AgNP coatings with different concentrations (0.2/1/5 mg/mL). (d) ATP activity inhibition rate of AgNP-GL13K coating at different temperatures (4 ℃ and room temperature). All data are presented as mean±SD (n=5). Using one-way ANOVA combined with Dunnett's post hoc test, * p<0.05 and * * p<0.01 indicate comparison with the control group

Antibacterial Activity

The results of in vitro antibacterial activity analysis of S. gordonii by different coatings are shown in Fig. 5. In Fig. 5 (a) and (b), the coating significantly reduces the CFU value of the bacteria (p<0.05). The single coating fails to significantly reduce the CFU values of bacteria and the difference is not statistically significant (p>0.05). In Fig. 5(c) and (d), ATP luminescence intensity has significant antibacterial activity. The difference is statistically significant (p<0.05) when compared with single coating. This result indicates that the AgNP-GL13K coating has significant antimicrobial effect against S. gordonii and is not significantly affected by AgNP concentration and coating temperature.

The results of in vitro antibacterial activity analysis of different coatings on P. aeruginosa and MRSA are shown in Fig. 6. In Fig. 6(a), the uncoated control titanium sheet has more P. aeruginosa bacteria attached to it, with a CFU value of 108. In contrast, the CFU value of P. aeruginosa bacteria on the single-coated titanium sheet is reduced to 106. After applying the coating, the CFU value of P. aeruginosa bacteria on the titanium sheet decreases to fewer than 104. Meanwhile, Fig. 6(b) shows that the antimicrobial properties of different coatings against MRSA bacteria exhibit a similar pattern. The coating has certain antimicrobial advantages.

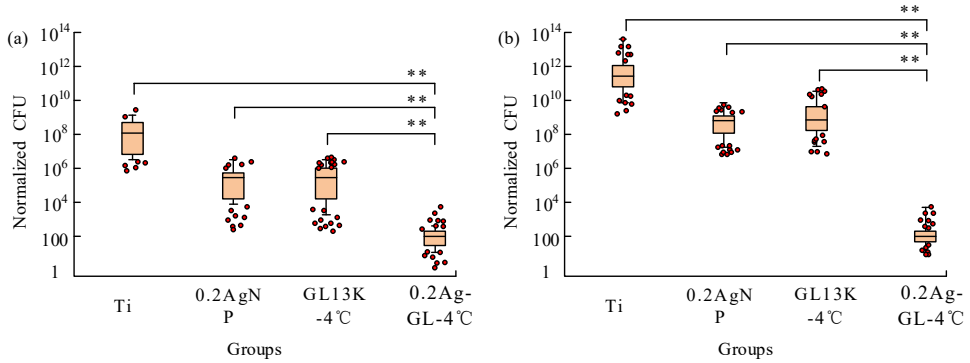

Fig. 6: Antibacterial Analysis of Drug-Resistant Bacteria. (a) Comparison of P.aeruginosa. (b) Comparison of MRSA. The data is expressed as mean±SD (n=5). **p<0.01 indicates comparison with the control group and each coating group, using Welch ANOVA+Dunnett T3 test

In Vitro Antimicrobial Analysis

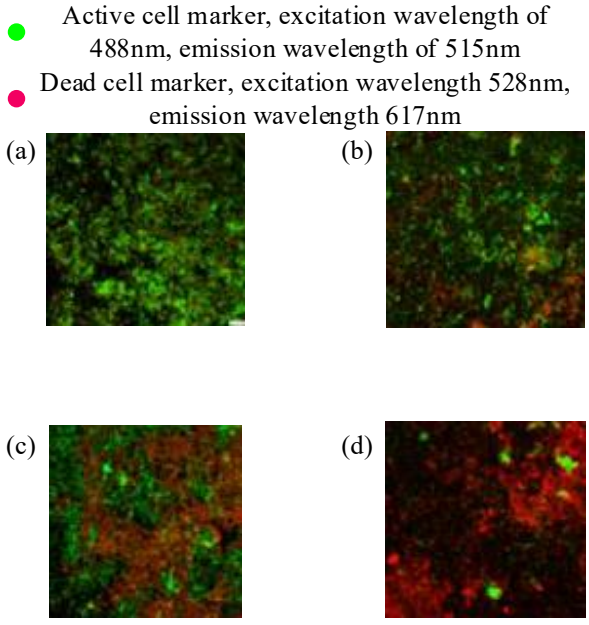

Fig. 7: Staining Experiment of Live/Dead Bacteria. (a) Titanium sheet. (b) 0.2mg/mLAgNP. (c) GL13K-4℃. (d) 0.2mg/mLAgNP-GL13K-4℃

DOI: 10.3844/ajbbsp.2026.22.01.015

The in vitro antimicrobial properties of 0.2 mg/mL AgNP loaded with GL13K at 4°C are studied and analyzed, and the experimental results are shown in Fig. 7. The control titanium sheet shows mainly green fluorescence under the control titanium sheet. Titanium sheets coated with AgNP-GL13K exhibit a large amount of red fluorescence, while those coated with AgNP exhibit a small amount. It can be concluded that the AgNP-GL13K coating has superior in vitro antimicrobial properties.

Cytocompatibility Analysis

The cells are in normal physiological state under fluorescence microscope observation, and no stress reaction is triggered by the coating material. Whereas the results of the quantitative cell proliferation test are shown in Fig. 8. The proliferation of human bone marrow MSCs on different groups of coatings under different incubation times does not have a significant gap. Moreover, the difference is not statistically significant ($p>0.05$). There is no effect of different coatings on the metabolic activity of human bone marrow MSCs, and the coatings have good biocompatibility.

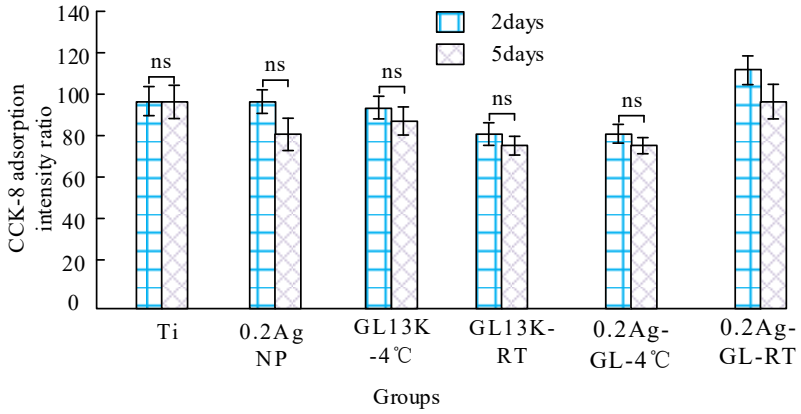

Fig. 8: Analysis of Cell Proliferation Ability. The CCK-8 method is used to detect cell viability (OD450 nm) after 1, 3, and 5 days of culture. The data is expressed as mean ± SD (n = 6). There is no statistically significant difference between the groups (p>0.05, mixed effects model)

Analysis of Antibacterial Activity in Vivo

In Fig. 9, the control titanium sheet has more MRSA bacteria attached to it with CFU values of 108 or more. In contrast, the CFU value of MRSA bacteria on the single coated titanium sheet is reduced to 107. The amount of bacteria attached to the single coating is reduced by a factor of 5-6. Whereas, the MRSA bacterial colonization of the coating is roughly around 104, which is about 100 times lower than the control coating. The coating has some in vivo antimicrobial advantages.

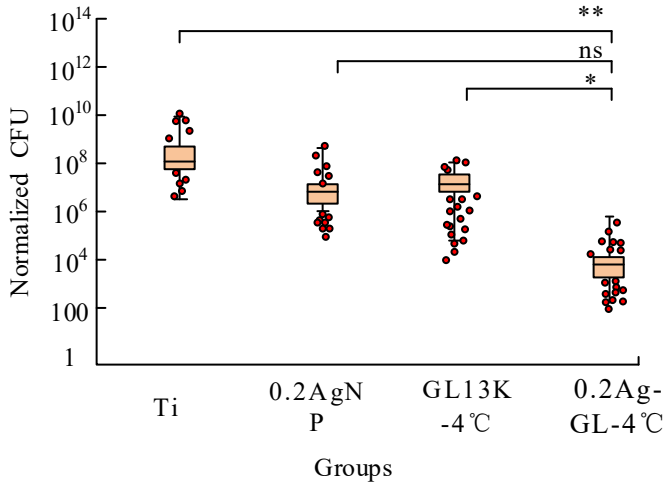

Fig. 9: Analysis of Antibacterial Activity in Vivo. The data is displayed as mean±SD (n=3). Statistical significance is evaluated using Kruskal Wallis test (non parametric) combined with Dunn's post hoc test. Compared with the uncoated control group, * p<0.05, * * p<0.01

DOI: 10.3844/ajbbsp.2026.22.01.015

Quantitative Analysis of Synergistic Effects

The microbroth dilution method is used for detection, and the MIC is used to evaluate and quantify the synergistic effects of the research methods. The results are shown in Table 2. It can be observed that for Gram positive bacterium S. gordonii, the MIC value of the coating (1.0±0.3 μg/mL) is reduced by 8 times and 16 times, respectively, compared to using AgNP alone (8.0±1.2 μg/mL) and GL13K alone (16.0±2.4 μg/mL). For the Gram-negative bacterium P. aeruginosa, the MIC value of the coating (4.0±0.6 μg/mL) is significantly lower than that of the individual components. The fractional inhibition concentration index is calculated to be 0.28 ($p<0.5$), further confirming the strong synergistic effect between AgNP and GL13K. These results are consistent with CFU and ATP detection data, indicating that the coating significantly improves antibacterial efficiency through a synergistic mechanism.

Table 2: Quantitative results of synergistic effects

Group	S. gordonii (μg/mL)	P. aeruginosa (μg/mL)
AgNP single use	8.0±1.2	32.0±4.8
GL13K single use	16.0±2.4	64.0±9.6
AgNP-GL13K	1.0±0.3*	4.0±0.6*

Note: * $p<0.05$ indicates comparison with a single group.

Discussion

Oral metal implant surgery was an important part of modern dentistry. It involved using metal implants to restore and improve patients' oral function and aesthetics [20, 21]. However, postoperative infection remained a key factor that affected both the success rate of surgery and the prognosis of patients. This issue deserved in-depth discussion by clinical experts. In oral metal implant surgery, the formation of biofilm had a serious impact on the implant and its surrounding tissues. The unique structure and composition of biofilms allow the bacteria within them to evade phagocytosis by host macrophages and resist the penetration of antimicrobial drugs. A great deal of research has been conducted on the development of single antimicrobial coatings. Although single-coated AMPs and AgNPs can reduce infection and inflammation to a certain extent and significantly inhibit bacteria, they still have some defects and shortcomings. Some specific types of bacteria may be resistant to single coatings. Prolonged or inappropriate use of a single coating may also lead to bacterial resistance. Moreover, some coatings can be toxic to host cells, affecting cell function and survival. Therefore, researchers have started to explore the possibility of combining the two. For example, Abdallah et al. used AgNPs in combination with nanocomposites [8]. Garibay-Alvarado et al. used AgNPs in combination with hydroxyapatite [10]. Alghofaily et al. used AgNPs in combination with calcium hydroxide to counteract Candida albicans infection [22]. In conclusion, the coatings demonstrated higher biosafety and antimicrobial activity due to their synergistic effects. In addition, the study's uniqueness lay in its use of electrostatic self-assembly technology to combine AgNP with GL13K. This technology achieves precise positioning at the nanoscale and significantly improving antibacterial performance. Previous studies have studied coatings combining AgNP with hydroxyapatite [10]. Although the method exhibited good antibacterial properties, it primarily relied on physical mixing and did not fully exploit the synergistic effects of AgNPs and AMPs. This study found that introducing GL13K improved the antibacterial effect of the coating and reduced the cytotoxicity of AgNPs at high concentrations. This study's coating exhibited a broader spectrum of antibacterial properties, particularly a stronger effect on Gram-negative bacteria, compared to the study by Abdallah et al. [8].

The stability results showed that GL13K formed stable nanofibers via a β-folding structure, which given it high stability under physiological conditions. By contrast, some natural AMPs, such as LL-37, were easily degraded by proteases, which resulted in poor stability when they were used in vivo. The GL13K protein formed a more stable β-folding structure at lower temperatures (4°C), helping it maintain its antibacterial performance when combined with AgNPs. The GL13K compound exhibited good antibacterial effects against various common oral bacteria, including both Gram-positive and Gram-negative bacteria. Compared with other AMPs, GL13K had a wider antibacterial spectrum. The combination of GL13K and AgNPs achieved precise nanoscale positioning through electrostatic self-assembly technology, which significantly improved antibacterial performance. This synergistic effect made GL13K superior to using AgNPs or GL13K alone in antibacterial efficacy. LL-37 was a well-studied natural AMP. However, it was unstable under physiological conditions and easily degraded by proteases. In contrast, GL13K exhibited better chemical stability by forming stable nanofibers through a β-folding structure.

HNP-1 was an AMP with good antibacterial activity against Gram-positive bacteria but poor activity against Gram-negative bacteria. In summary, coatings could achieve more efficient antibacterial effects.

The mechanism of synergistic effect could be derived from this. First, AgNPs and GL13K were combined using electrostatic self-assembly technology to precisely position the AgNPs on the GL13K nanofibers. This combination not only improved the distribution uniformity of AgNP, but also enhanced its contact efficiency with bacteria. Therefore, it could significantly improve its antibacterial performance. AgNPs primarily damaged bacterial cell membranes and DNA by releasing silver ions. GL13K, on the other hand, bound to bacterial cell membranes through its cationic properties, thereby disrupting membrane integrity. Combining the two enhanced the antibacterial effect of AgNP, which increased the destructive effect of GL13K on bacterial cell membranes, achieving synergistic antibacterial activity. In addition, GL13K could form a more ordered antiparallel β-folding structure under low-temperature conditions. This structure enhanced the stability of GL13K and provided a more stable binding site for AgNP. This maintained efficient antibacterial performance under physiological conditions. In terms of biocompatibility, the nanofiber structure of GL13K could encapsulate AgNPs, thereby reducing their toxicity to cells at high concentrations. This wrapping effect not only reduced the direct damage of AgNP to cells, but also improved the overall biocompatibility of the coating. Meanwhile, coatings formed by electrostatic self-assembly had good surface properties and biocompatibility. These coatings could better simulate the microenvironment of living organisms and promote cell adhesion and proliferation. GL13K's cationic properties enabled it to interact with negative charges on the cell surface, thereby enhancing the cell's adhesion ability.

The research results guaranteed the long-term stability and safety of oral implants, providing a theoretical basis and technical support for developing efficient, safe, and durable antibacterial oral materials. However, the research has limitations because it do not evaluate the coating's long-term durability, which may affect its clinical application feasibility. Therefore, future research should include clinical translational studies that evaluate the effect of the coating's actual application in oral implants. These studies should provide strong support for the clinical use of the coating.

Conclusion

A new dual-effect antibacterial coating was developed by combining GL13K and AgNPs through electrostatic self-assembly technology. The experimental results showed that: 1) The coating exhibited significant antibacterial activity against both Gram-positive and Gram-negative bacteria, including streptococcus pyogenes, pseudomonas aeruginosa, and MRSA. The bacterial CFU were reduced by 100 times ($p<0.05$) compared to single component coatings. Moreover, the MIC was reduced by 8-16 times. 2) The precise positioning of AgNPs was achieved using β-folded nanofiber structures, which solved the problem of uneven distribution caused by traditional physical mixing methods. Additionally, low temperature (4 ℃) conditions could enhance structural stability. 3) Cell experiments confirmed that the coating did not affect the proliferation activity of human bone marrow mesenchymal stem cells ($p>0.05$). This result overcome the problem of high concentrations of AgNPs causing cytotoxicity. Compared to previous studies, these studies simply mixed AgNPs with materials such as hydroxyapatite. This study aims to utilize the electrostatic interaction between the GL13K polar end and silver nanoparticles to achieve nanoscale ordered assembly. This improves antibacterial efficiency, and prolong the reaction time. However, the research has limitations because it did not evaluate the coating's long-term durability, which may affect its clinical application feasibility. Therefore, future research should include clinical translational studies to evaluate the coating's actual application effect in oral implants and provide strong support for its clinical use.

Acknowledgment

Thank you to the publisher for their support in the publication of this research article. We are grateful for the resources and platform provided by the publisher, which have enabled us to share our findings with a wider audience. We appreciate the efforts of the editorial team in reviewing and editing our work, and we are thankful for the opportunity to contribute to the field of research through this publication.

Funding Information

This study has not received any external funding.

Author Contributions

Yanli Lv: Writing original draft preparation, writing review and editing, formal analysis, data curation.

Weikai Zhang: Software, formal analysis, writing, review and editing. All authors read and approved the final manuscript.

Ethics

This study is reviewed and approved by the Institutional Animal Care and Use Committee (IACUC) of Luoyang Polytechnic (approval ID: LPEC-2416). It complies with the 3Rs principles and the ARRIVE guidelines.

Data Availability Statement

The datasets used and/or analysed during the current study available from the corresponding author on reasonable request.

Conflicts of Interest

No conflict of interest exists in the submission of this manuscript.

References

1. Im S, Lee J H, Shim Y S. Antimicrobial peptides targeting oral pathogens: Applicability as an oral disease treatment and dental material. Journal of Dental Hygiene Science, 2024, 24(4): 231-248.
2. Nireeksha, Hegde M N, Kumari N S. Potential role of salivary vitamin D antimicrobial peptide LL-37 and interleukins in severity of dental caries: an exvivo study. BMC Oral Health, 2024, 24(1): 79-88.
3. Campos J, Pires M F, Sousa M, Campos, C., da Costa, C F F A, Sampaio-Maia B. Unveiling the relevance of the oral cavity as a Staphylococcus aureus colonization site and potential source of antimicrobial resistance. Pathogens, 2023, 12(6): 765-774.
4. Zhang L, Zhang P, Song X, She P, Liu K, Song W, Liu L. “Cofactor Corona” Equipped gold nanozyme: From enhancing catalytic activity to oral cavity application. Chemistry of Materials, 2024, 36(17): 8378-8390.
5. Xin Q, Zhang Y, Yu P, Zhao Y, Sun F, Zhang H, Li J. Oral environment-adaptive peptide–polymer conjugate for caries prevention with targeting, antibacterial, and antifouling abilities. Chemistry of Materials, 2024, 36(3): 1691-1706.
6. Grachev D I, Martynenko A V, Perekhodov S N, Kostyrin E V, Mustafaev M S, Akhmedov K G, Deshev A V, Rozanov D G, Korotkova N L, Kerasov S N, Arutyunov S A. New Assessment Model of Financing Treatment of Patients with Complete Tooth Loss. Emerging Science Journal, 2024, 8(5): 1898-1916.
7. Snauwaert J, Vanhoucke M. A classification and new benchmark instances for the multi-skilled resource-constrained project scheduling problem. European Journal of Operational Research, 2023, 307(1): 1-19.
8. Abdallah O M, Sedky Y, Shebl H R. Comprehensive evaluation of the antibacterial and antibiofilm activities of NiTi orthodontic wires coated with silver nanoparticles and nanocomposites: an in vitro study. BMC Oral Health, 2024, 24(1): 1345-1360.
9. Elchaghaby M A, Rashad S, Wassef N M. Bioactivity and antibacterial effect of star anise biosynthesized silver nanoparticles against Streptococcus mutans: an in vitro study. BMC Complementary Medicine and Therapies, 2024, 24(1): 259-267.
10. Garibay-Alvarado J A, Garcia-Zamarron D J, Silva-Holguín P N, Donohue-Cornejo A, Cuevas-González J C, Espinosa-Cristóbal L F, Reyes-López, S Y. Polymer-based hydroxyapatite–silver composite resin with enhanced antibacterial activity for dental applications. Polymers, 2024, 16(14): 2017-2025.
11. Shen, Q., Zhu, H., Zhou, H., Jiang, T., & Liu, Y. (2023). Preparing and antimicrobial activity of hydrogel with biosynthesized silver nanoparticles using Carex Meyeriana Kunth. American Journal of Biochemistry and Biotechnology, 19(2), 138–145. https://doi.org/10.3844/ajbbsp.2023.138.145
12. Ekrikaya S, Yilmaz E, Arslan S, Karaaslan, R., Ildiz, N., Celik, C, Ocsoy I. Dentin bond strength and antimicrobial activities of universal adhesives containing silver nanoparticles synthesized with Rosa canina extract. Clinical Oral Investigations, 2023, 27(11): 6891-6902.
13. Elmoghazy Y, Abuelgasim E M O, Osman S A. Effective mechanical properties evaluation of unidirectional and bidirectional composites using virtual domain approach at microscale. Archives of Advanced Engineering Science, 2023, 1(1): 27-37.
14. Yang Y, Qian Y, Zhang M, Hao S, Wang H, Fan Y, Wang F. Host defense peptide-mimicking β-peptide polymer displaying strong antibacterial activity against cariogenic Streptococcus mutans. Journal of Materials Science & Technology, 2023, 133(1): 77-88.
15. Rapala-Kozik M, Surowiec M, Juszczak M, Wronowska E, Kulig K, Bednarek A, Kozik A. Living together: The role of Candida albicans in the formation of polymicrobial biofilms in the oral cavity. Yeast, 2023, 40(8): 303-317.
16. Chen M A, Yang Y H, Liu C K, Matsuo K, Hsu C C, Lin Y C, Huang H L. Salivary antimicrobial peptide in patients with dementia before and after clinical oral rehabilitation programme: A randomised controlled trial. Journal of Oral Rehabilitation, 2025, 52(1): 1-8.
17. Stewart L J, Hong Y J, Holmes I R, Firth S J, Ahmed Y, Quinn J, Djoko K Y. Salivary antimicrobial peptide histatin-5 does not display Zn (II)-Dependent or-independent activity against streptococci. ACS Infectious Diseases, 2023, 9(3): 631-642.

18. Ito R, Uchino T, Uchida M, Fujie S, Iemitsu K, Kojima C, Iemitsu M. Acute salivary antimicrobial peptide secretion response to different exercise intensities and durations. American Journal of Physiology-Regulatory, Integrative and Comparative Physiology, 2024, 327(6): 616-622.
19. Blancas-Luciano B E, Zamora-Chimal J, da Silva-de Rosenzweig P G, Ramos-Mares M, Fernández-Presas A M. Macrophages immunomodulation induced by Porphyromonas gingivalis and oral antimicrobial peptides. Odontology, 2023, 111(4): 778-792.
20. Zulfikar T, Siregar T N, Rozaliyani A, Sutriana A. Antimicrobial Potential of Calotropis gigantea Leaf Against Klebsiella pneumoniae in Ventilator-Associated Pneumonia. Journal of Human, Earth, and Future, 2024, 5(3): 456-470.
21. Zahara E, Balqis U, Soraya C. The Potential of Ethanol Extract of Aleurites Moluccanus Leaves as TNF-α Inhibitor in Oral Incision Wound Care Model. Journal of Human, Earth, and Future, 2024, 5(4): 674-687.
22. Alghofaily, M., Alfraih, J., Alsaud, A., Almazrua, N., Sumague, T. S., Auda, S. H., & Alsalleeh, F. (2024). The Effectiveness of Silver Nanoparticles Mixed with Calcium Hydroxide against Candida albicans: An Ex Vivo Analysis. Microorganisms, 12(2), 289. https://doi.org/10.3390/microorganisms12020289